3D MODEL ANALYSIS OF EXISTING CT SYNDESMOSIS MEASUREMENTS

Thomas Ebinger, MD, Jess Goetz, PhD, Lori Dolan, PhD, Phinit Phisitkul, MD

ABSTRACT

Introduction: Use of Computed Tomography (CT) to evaluate syndesmotic reduction following injury has significantly increased in recent years. The aim of this study was to compare existing clinical measurements of syndesmotic reduction to gold standard measurements of fibular motion obtained from a full 3D model.

Methods: Three common clinical measures for assessing syndesmotic congruity on axial CT slices were identified in the literature. Each measure was manually performed on 170 cadaveric ankle CT scans obtained with variable degrees of simulated syndesmotic displacement. Clinical measures were assessed for intraobserver and interobserver reliability and compared to objective measures of true medial/lateral and anterior/posterior translation and fibular rotation that were obtained from a 3D model. Pearson correlation coefficients (PCC) were computed to determine which clinical measurements were most accurate for describing syndesmotic motion obtained from the 3D model.

Results: All three clinical measurement techniques demonstrated good to excellent interobserver and intraobserver reliability. Medial/lateral displacement of the fibula was best correlated with the difference between the anterior and posterior tibiofibular joint space measurements described by Elgafy et al (PCC = 0.29 small correlation). Anterior/posterior displacement of the fibula was well correlated with the anterior/posterior measurement described by Phisitkul et al (PCC = 0.69 large correlation). Fibular rotation was best correlated with the average of the Elgafy anterior and posterior tibiofibular joint space measurements (PCC=0.33, moderate correlation). Proximal/distal displacement of the lateral malleolus was best correlated with the Elgafy posterior tibiofibular joint space measurement (PCC=0.49, moderate correlation).

Discussion: While the clinical measurements were adequately reproducible, they showed only moderate to small correlations with the 3D measurements of movement of the fibula in the longitudinal, medial/lateral or rotational directions. The only fibular translation measured by the 3D model that was well described by the three clinical measures was fibular movement in the anterior/posterior direction. This work demonstrates a need for improved clinical measurements of syndesmotic congruity on axial CT scans to serve as surrogates for the true movement of the fibula.

INTRODUCTION

Small changes in ankle joint congruity, including the syndesmosis, have been shown to have large effects on joint contact stresses[1,2]. The ramifications of these changes in contact stresses are thought to be related to the high rate of post traumatic osteoarthritis in the ankle joint. Radiographs have been shown to have limited sensitivity in detecting subtle syndesmosis and ankle joint malalignments and are highly sensitive to positional change[3,4]. Consequently, the use of Computed Tomography (CT) in the evaluation of ankle injury has greatly increased in recent years. The advantages of CT-based evaluation of the syndesmosis are that unlike plain radiographs, CT provides axial views of the syndesmosis and CT is substantially less dependent on ankle positioning at the time of imaging[5,6,3]. This improved visualization has shown high rates of syndesmotic malreduction on CT following open reduction internal fixation of ankle fractures[6, 7]. Many of these malreductions go undetected on plain radiographs, meaning subtle malreductions may go unidentified without advanced imaging[8, 9].

The manner in which the syndesmosis is evaluated using CT has been highly variable. Several different methods have been used to describe the distal tibia-fibula relationship in both injured and uninjured ankles using manual measurements between anatomic landmarks, and several studies have used only subjective criteria[6, 10-14]. In all cases, evaluation of the syndesmosis is made on a single axial slice through the volume, neglecting

Corresponding Author:
Thomas Ebinger, MD
University of Iowa
Department of Orthopaedics and Rehabilitation
200 Hawkins Drive
Iowa City, IA 52242
thomas-ebinger@uiowa.edu

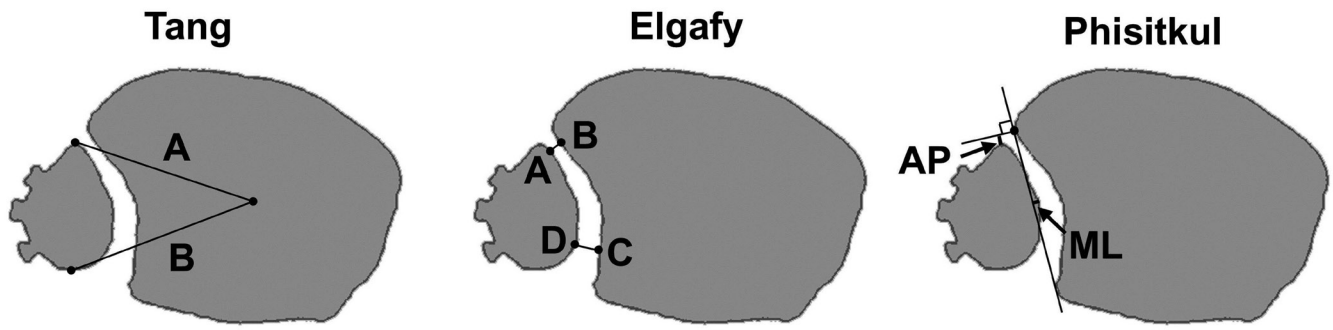

Figure 1. Clinical measurements made manually on CT scans and calculated automatically by the computer algorithm. Measurements are shown on 2D cross-sections through the segmented 3D volume and the irregularities in the fibular contour are screw heads used to ensure consistent clamp placement for scanning. The Tang measurement is expressed as A/P, and indicates a measure of fibular rotation. The Elgafy measurements and the Phisitkul measurements indicate fibular translation.

available 3D information. Although several methods have been shown to be reproducible in their application, their validity in assessing movement of the fibula relative to the tibia has not been shown. It is unclear if the 2D measurement methods used clinically for CT evaluation accurately represent the true deviations in the distal tibia-fibula relationship.

The purpose of this study was to evaluate existing, clinically applicable CT measurements of the syndesmosis against objective, automatically calculated gold-standard measurements taken from the calibrated 3D CT volume. While it would be ideal to always obtain fully objective 3D data about tibia and fibula position from a CT scan, this requires clinically unrealistic, time-consuming segmentation, modeling, and analysis. The goal of this work was to identify which of the commonly employed clinical measures were most indicative of true fibular motion relative to the tibia in cases of a disrupted syndesmosis.

MATERIALS AND METHODS

Ten through-the-knee lower extremity cadavers were used in the study. In order to create variability in the syndesmosis joint and relative positions of the tibia and fibula, various degrees of syndesmotic instability ranging from an isolated rupture of the anterior inferior tibiofibular ligament to a complete disruption of the syndesmosis with posterior malleolar fracture and deltoid ligament disruption were created using a scalpel under direct visualization. In each disrupted condition reduction forceps were applied to the medial and lateral malleoli at one centimeter above the joint line in three different orientations (anteromedial to posterolateral, medial to lateral, and posteromedial to anterolateral). Marking screws were placed in each specimen to ensure reproducible clamp placements and manipulations. A total of 170 CT scans (17 per specimen) were evaluated.

Manual Clinical Measurements

Common clinical measurement techniques used in this work included a metric described by Tang et al[15]. intended to describe fibular rotation, measurement of anteroposterior and mediolateral fibular displacement described by Phisitkul et al[16]., and a measurement of the syndesmotic joint space described by Elgafy et al[13]. (Figure 1). The Tang measurement was made by finding the ratio of the vectors directed from the tibial centroid to the anterior-most point on the fibula and from the tibial centroid to the posterior-most point on the fibula. The anterior Elgafy measurement was made between the closest point on the anterior tubercle of the tibia and the point on the fibula closest to that location. The posterior Elgafy measurement was made between the point on the fibula that was midway between the medial-most and the posterior-most points, and the location on the tibia that was closest to that location. The difference and average between the anterior and posterior Elgafy measurements was calculated[14]. The medial Phisitkul measurement was made between a line connecting the anterior and posterior tubercles of the tibia, and the medial-most border of the fibula. The anterior Phisitkul measurement was made between the line perpendicular to the line connecting the tubercles at the anterior tubercle, and the anterior-most point of the fibula.

These measures were performed manually on 2D axial CT slices using Vitrea® software (Vital Images, Minnetonka, MN, USA). Two observers not involved in the specimen preparation made measurements separately and in the exact manner described in the articles referenced. Measurements were repeated 12 weeks later and inter-rater reliability and intra-rater reliability was assessed.

Objective Geometric Measurements

To obtain objective measurements of fibula motion relative to the tibia, 3D models were generated from

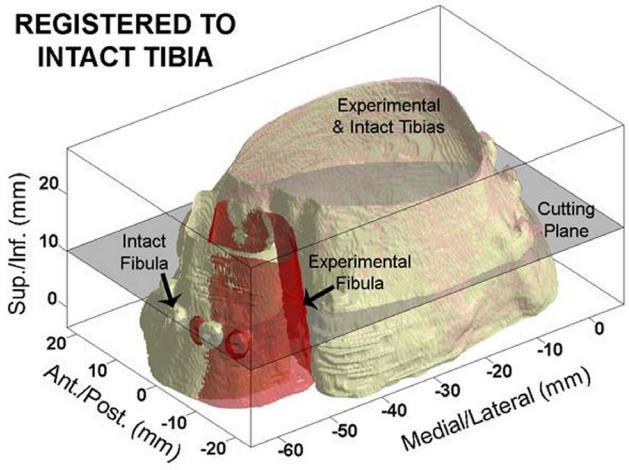

Figure 2. Illustrative example of the 3D surfaces generated by segmentation. The tibia in the experimental case has been aligned with the intact tibia using the iterative closest point algorithm. The movement of the fibula resulting from clamping the fibula with a posteriorly directed force can be seen by the offset of the experimental fibula (red) from the intact fibula (bone). The 2D cutting plane 10mm above the articular surface for extracting the cross section from which the objective 2D measurements were made is shown for reference.

each of the 170 CT scans. 3D models were generated by segmentation of the tibia and the fibula using a custom routine developed in Matlab (The Mathworks, Natick, MA, USA). The routine consisted of a custom-written version of a Chan-Vese active contouring algorithm to automatically detect the outer edges of cortical bone, followed by an optional manual editing step to ensure accurate boundary identification. Approximately 25mm of tissue proximal to the distal tibial articular surface was segmented for this work.

Segmentations from the intact case of each specimen were rotated into a specimen-specific anatomic coordinate system developed from bony landmarks that were identified during the segmentation process. During segmentation of the intact condition for each of the ten specimens, the distal-most medial and lateral malleolus points, and the level of the central distal tibial surface were manually selected. All segmentation data were translated so that the origin of the coordinate system was at the AP/ML location of the medial malleolus and at the level of the distal tibial articular surface in the proximal/distal direction. The specimen specific x-axis was defined by the vector from the medial to the lateral malleolus, the y-axis was defined perpendicular to the x-axis and directed along the shaft of the tibia, and the z-axis was defined with the cross-product of the x- and y-axes. Translating the 3D models into a coordinate system defined by bony landmarks removed any effects of specimen positioning in the scanner on the resulting syndesmotic measurements.

An iterative closest point algorithm was then used to match the surfaces of each experimental tibia segmentation to its anatomically aligned intact tibia segmentation. Next, a 2D cross-section through the aligned 3D volumes was selected at a level 10mm proximal to the distal tibial articular surface (Figure 2). This cross section was selected to correspond to the level above the joint that was evaluated in manual measurements on the 2D axial CT section. On each cross section extracted from the 3D model, the three clinical measurements (Tang, Elgafy, and Phisitkul measurements) and four objective 2D measurements were made using a fully automated custom Matlab algorithm.

The three clinical measurements were made by the algorithm using the same anatomic landmarks that were manually identified on the 2D axial CT slices. However, because the algorithm identified these landmarks from the 2D cross section obtained from the 3D model, these clinical measures were automated, perfectly repeatable, and user independent to serve as a gold standard. In addition to the basic clinical measurements, two derived measures were also evaluated. The difference between the anterior and posterior Elgafy measurements was calculated as a potential measure of fibular rotation, and the average of the anterior and posterior Elgafy measurements was calculated as a potential measure of medial/lateral fibular movement.

The objective measurements made by the algorithm consisted of 1) medial/lateral movement of the fibular centroid 10mm proximal to the distal tibial articular surface, 2) anterior/posterior movement of the fibular centroid 10mm proximal to the distal tibial articular surface, 3) internal/external rotation of the fibula around its own proximal/distal axis, and 4) internal/external rotation of the fibula around the tibial proximal/distal axis (Figure 3). The medial/lateral and anterior/posterior movements of the fibula were differences between the centroid of the fibula in the experimental condition relative to the location of the centroid in the intact condition. Rotation of the fibula was calculated by the angular change in a vector from the centroid of the fibula to the anterior-most point on the fibula in the intact case, to a vector from the fibula centroid to that same point in the experimental condition. Rotation around the tibia was calculated by the angular rotation of the fibula centroid around the tibial centroid.

Additionally, to investigate fibular movements out of the axial plane of the CT or cross-sectional data, movement of the distal lateral malleolus was followed in the full 3D segmentation data. First, an iterative closest point algorithm was used to determine the transformation required to move the fibula from its intact position into a given experimental position. The original lateral malleolus point was prescribed that same transformation,

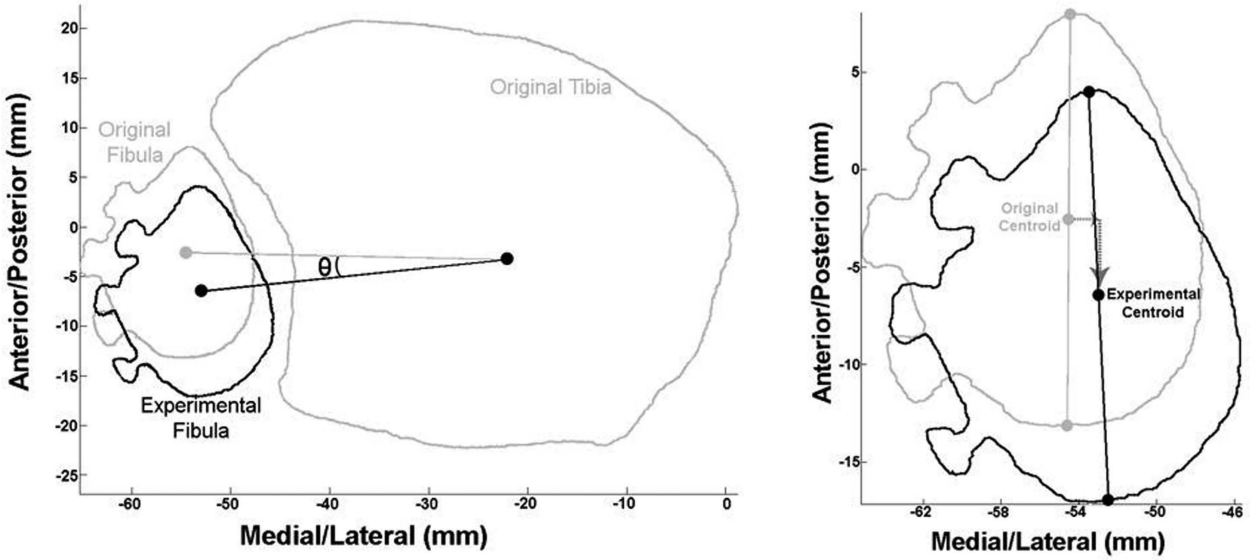

Figure 3. Objective measurements of fibular movement made by the algorithm in the 2D cutting plane. The rotation of the fibula (θ on the Left) around the tibia was calculated as the angle between vectors directed from the tibial centroid to the centroid of the fibula under different clamping conditions. The medial/lateral and anterior/posterior movement of the fibular centroid was calculated directly (Right), and the rotation of the fibula around its own axis was calculated by the angle between the lines connecting the anterior-most and posterior-most fibular points in the different clamping conditions.

and the resulting displacements of the lateral malleolus were calculated as the difference from the location of the original lateral malleolus point.

STATISTICAL ANALYSIS

The reliability of the manual clinical measurements was assessed using interclass correlation coefficients (ICC)[17,16,1]. The interclass correlation coefficient was calculated and compared between the two different observers (inter-rater reliability) and between repeated measurements by each of the two observers (intra-rater reliability) for each of the measurements. ICC was defined as poor (<0.40), good (0.41-0.75), or excellent (>0.76)[17]. The relationship between the manual clinical measurements and the objective geometric measurements made from the 3D model was assessed using Pearson Correlation Coefficients (PCC). PCCs were calculated between each manual clinical 2D measurement and each algorithm derived objective measurement. The PCC interpreted as small (0.1-0.3), moderate (0.3-0.5), large (0.5-0.7) or very large (>0.7)[18].

RESULTS

Interclass correlation coefficients for the manual clinical 2D measurements are reported in Table 1. Both inter-rater and intra-rater reliability was found to be good to excellent for all measurements. The measurement with the highest ICC overall was the Phisitkul AP measurement. The lowest overall ICC was found with the Tang et al. rotational measurement.

Pearson correlation coefficients between the computer algorithm-generated clinical measurements and the objective 3D-based geometric measurements are shown in Table 2. Actual mediolateral displacement of the fibula was best correlated with the difference between the anterior and posterior tibiofibular joint space measurements using Elgafy method (PCC = 0.29, small correlation). Anteroposterior displacement of the fibula was best correlated with the Phisitkul anteroposterior measurement method (PCC = 0.69, large correlation). Rotational displacement of the fibula around its own axis best correlated with the average between Elgafy anterior and Elgafy posterior measurements (PCC = 0.33, moderate correlation). Longitudinal displacement of the lateral malleolus was best correlated with the Elgafy posterior tibiofibular joint space measurement (PCC=0.49, moderate correlation).

DISCUSSION

With the increasing use of CT for syndesmosis evaluation, several attempts have been made to establish techniques for describing anteroposterior, mediolateral, and rotational changes of the syndesmosis on axial CT slices. Although there is no consensus on one set of measurements that provides a gold-standard assessment of syndesmosis congruity, it is clear that previously described methods for manually measuring the syndesmosis on axial CT slices are reproducible. This reproducibility was reported in the papers originally describing the measurement techniques by Elgafy, Tang, and

Interclass Correlations of CT syndesmosis measurements		
Group	Inter-rater ICC*	Intra-rater ICC*
Elgafy		
Anterior Measurement	0.94	0.81
Posterior Measurement	0.43	0.44
Tang	0.71	0.53
Phisitkul		
AP measurement	0.92	0.97
ML measurement	0.80	0.71
*ICC = Interclass Correlation (<0.40 poor, 0.40-0.75 good, >0.75 excellent)		

Table 1. Interclass correlation coefficients for manual clinical measurements. All measurements demonstrated good to excellent correlation in inter-rater and intra-rater testing with the exception of the Elgafy posterior (C-D) measurement.

Measurement	3D Model ML	3D Model AP	3D Model Rotation	3D Model Longitudinal
Phisitkul ML	-0.026	0.260	-0.282	-0.135
Phisitkul AP	0.025	**-0.689**	0.275	-0.013
Tang Rotational	-0.060	-0.361	0.055	0.152
Elgafy Anterior	-0.119	**0.591**	-0.192	0.037
Elgafy Posterior	***-0.298***	-0.095	0.008	***0.499***
Elgafy (A-P)	***-0.298***	**0.611**	-0.046	0.171
Elgafy A/P Avg	0.281	0.173	***-0.332***	-0.229

Table 2. Pearson correlation coefficients calculated between described measurment techniques using bony landmarks and computer generated measurments tracking centroids of the tibia and fibula. The AP measurement was well described by the Phisitkul AP, Elgafy anterior, and the Elgafy A-P measurements (bold). The remaining translations and rotations were only moderately well described by perturbations of the Elgafy measurements (bold italics).

Phisitkul, and was reproduced in this work as indicated by all measurements demonstrating good to excellent interclass correlation coefficients.

Each of the clinical measurements is based on specific anatomic landmarks which are easily discernible even in cases of a malaligned syndesmosis. However, these measurements are limited to the axial plane, and changes in the measurements represent some combination of fibular translation and rotation. Obtaining pure translational and rotational information for the fibula, which were the objective measures in this work, requires development and analysis of a 3D model. While the 3D model provides the most definitive information, it is prohibitively slow for regular implementation in clinical evaluation of CT scans. Therefore it is highly desirable to know which of the clinical measures best represents the true movement of the fibula relative to the tibia.

Unfortunately, little correlation was found between many of the clinical measurements and the objective geometric measures taken from the 3D model. Anteroposterior movement of the tibia-fibula syndesmosis relationship correlated well with several of the clinical measurement techniques, most significantly with the Phisitkul A-P measurement. However, the geometric movement of the tibia-fibula relationship in the mediolateral, the longitudinal, and the rotational planes was not found to correlate significantly with any of the clinical measurement techniques. Typically, the anterior-posterior plane is the most problematic when attempting to achieve anatomic reduction of the syndesmosis[15,19,6,7,20]. Therefore, it is encouraging that according to our work this plane can be adequately measured using one of several clinical measurements. However, syndesmotic congruity in the mediolateral, longitudinal, and rotational planes is also important and true fibular movement in these planes is inadequately assessed using clinical measurements on 2D axial CT slices.

This study does come with limitations. The cadaveric model employed to simulate the injury may not truly replicate the clinical setting because the CT scans of the ankles were obtained with reduction forceps applying a compressive force. This resulted in none of the specimens having a large diastasis of the syndesmosis. Additionally, there was no fibular fracture simulated in

this mode, therefore this work presumed perfect reduction of the fibula in a clinical setting. Because of the compressive force applied in the model and the lack of fibula fracture, the translational and rotational measurements obtained by all methods were small. This could have led to range restriction when assessing correlation coefficients.

A further limitation of this work relates to application of the clinical measurements used in this work. In the clinical (rather than in the research) setting, the Elgafy and Phisitkul measurements are limited to ankles without a posterior malleolus fracture. This is because in the case of the Phisitkul measurement, reference line A is dependent on an intact fibular incisura, and the Elgafy posterior measurement (CD) depends on a non-displaced posterior incisura. Advantages of the Elgafy and Phisitkul measurements are that they may be done quickly. This is not the case for the Tang measurement of rotation as finding the center of the tibia by the method described can be quite cumbersome.

Although it would be ideal to use advanced analysis of 3D imaging techniques routinely, this is not practical in the clinical setting. Yet, based on our findings that current clinical measurements of syndesmosis congruity do not correlate strongly with mediolateral, longitudinal, and rotational movement of the fibula, we feel that improved clinical measurements are needed for useful clinical application of CT data in assessment of the syndesmosis. Future clinical measurement techniques should be validated as they arise to ensure accurate evaluation of syndesmosis motion on axial CT scans. To date, most 2-D measurement techniques have focused on measuring the syndesmosis using the axial cuts of the CT scan. It is likely that improvements in assessing the longitudinal and possibly rotational changes in the syndesmosis would be better assessed on a coronal plane CT view.

REFERENCES

1. **McKinley TO, Rudert MJ, Tochigi Y, Pedersen DR, Koos DC, Baer TE, et al.** Incongruity-dependent changes of contact stress rates in human cadaveric ankles. J Orthop Trauma 2006 Nov-Dec;20(10):732-8.
2. **Tochigi Y, Rudert MJ, McKinley TO, Pedersen DR, Brown TD.** Correlation of dynamic cartilage contact stress aberrations with severity of instability in ankle incongruity. J Orthop Res 2008 Sep;26(9):1186-93.
3. **Beumer A, van Hemert WL, Niesing R, Entius CA, Ginai AZ, Mulder PG, et al.** Radiographic measurement of the distal tibiofibular syndesmosis has limited use. Clin Orthop Relat Res 2004 Jun;(423)(423):227-34.
4. **Brage ME, Bennett CR, Whitehurst JB, Getty PJ, Toledano A.** Observer reliability in ankle radiographic measurements. Foot Ankle Int 1997 Jun;18(6):324-9.
5. **Saldua NS, Harris JF, Leclere LE, Girard PJ, Carney JR.** Plantar flexion influences radiographic measurements of the ankle mortise. J Bone Joint Surg Am 2010 Apr;92(4):911-5.
6. **Gardner MJ, Demetrakopoulos D, Briggs SM, Helfet DL, Lorich DG.** Malreduction of the tibiofibular syndesmosis in ankle fractures. Foot Ankle Int 2006 Oct;27(10):788-92.
7. **Rammelt S, Zwipp H, Grass R.** Injuries to the distal tibiofibular syndesmosis: an evidence-based approach to acute and chronic lesions. Foot Ankle Clin 2008 Dec;13(4):611,33, vii-viii.
8. **Miller AN, Carroll EA, Parker RJ, Boraiah S, Helfet DL, Lorich DG.** Direct visualization for syndesmotic stabilization of ankle fractures. Foot Ankle Int 2009 May;30(5):419-26.
9. **Park JC, McLaurin TM.** Acute syndesmosis injuries associated with ankle fractures: current perspectives in management. Bull NYU Hosp Jt Dis 2009;67(1):39-44.
10. **Taser F, Shafiq Q, Ebraheim NA.** Three-dimensional volume rendering of tibiofibular joint space and quantitative analysis of change in volume due to tibiofibular syndesmosis diastases. Skeletal Radiol 2006 Dec;35(12):935-41.
11. **Dikos GD, Heisler J, Choplin RH, Weber TG.** Normal tibiofibular relationships at the syndesmosis on axial CT imaging. J Orthop Trauma 2012 Jul;26(7):433-8.
12. **Ebraheim NA, Lu J, Yang H, Mekhail AO, Yeasting RA.** Radiographic and CT evaluation of tibiofibular syndesmotic diastasis: a cadaver study. Foot Ankle Int 1997 Nov;18(11):693-8.
13. **Elgafy H, Semaan HB, Blessinger B, Wassef A, Ebraheim NA.** Computed tomography of normal distal tibiofibular syndesmosis. Skeletal Radiol 2009 Oct 15.
14. **Mukhopadhyay S, Metcalfe A, Guha AR, Mohanty K, Hemmadi S, Lyons K, et al.** Malreduction of syndesmosis–are we considering the anatomical variation? Injury 2011 Oct;42(10):1073-6.
15. **Tang CW, Roidis N, Vaishnav S, Patel A, Thordarson DB.** Position of the distal fibular fragment in pronation and supination ankle fractures: a CT evaluation. Foot Ankle Int 2003 Jul;24(7):561-6.
16. **Phisitkul P, Ebinger T, Goetz J, Vaseenon T, Marsh JL.** Forceps Reduction of the Syndesmosis in Rotational Ankle Fractures. JBJS 2012(December 2012):pending publication.

17. **Shrout PE, Fleiss JL.** Intraclass correlations: uses in assessing rater reliability. Psychol Bull 1979 Mar;86(2):420-8.
18. **Shoukri MM, Pause CA.** Statistical methods for health sciences. 2nd ed. Boca Raton, Fla.: CRC Press; 1999.
19. **Tornetta P,3rd, Spoo JE, Reynolds FA, Lee C.** Overtightening of the ankle syndesmosis: is it really possible? J Bone Joint Surg Am 2001 Apr;83-A(4):489-92.
20. **Miller AN, Barei DP, Iaquinto JM, Ledoux WR, Beingessner DM.** Iatrogenic Syndesmosis Malreduction Via Clamp and Screw Placement. J Orthop Trauma 2012 Apr 28.